Multiple-order Raman scattering in MnO_4^{2-}-doped CsI

T. P. Martin and S. Onari†
Max-Planck-Institut für Festkörperforschung, Stuttgart, Federal Republic of Germany
(Received 23 August 1976)

Multiple-order Raman scattering was observed in CsI doped with MnO_4^{2-}. The Raman spectra consist of a series of sharp, equally spaced lines due to multiple-order scattering from the totally symmetric mode of MnO_4^{2-}. Each sharp line in the Raman spectra exhibits a side band which is composed partly of low-frequency CsI phonons and partly of high-frequency internal vibrations of the MnO_4^{2-} molecule. The intensity of the Raman scattering was measured as a function of laser frequency. In general, the Raman scattering was seen to be enhanced each time the laser frequency was tuned to one of the vibrational sublevels of the excited electronic state. An exception occurred at the third vibronic level at which a minimum in the scattered intensity was observed. The Raman spectra, resonance enhancement spectra, and optical absorption spectra can be explained, quantitatively, using a simple model involving a ground electronic state and one excited electronic state each with vibronic structure corresponding to one localized mode of vibration. Since the frequency of this localized mode is shown to be different in the ground and excited electronic states, we can easily distinguish between resonant Raman scattering and hot luminescence.

I. INTRODUCTION

During the past few years there has been considerable discussion concerning the nature of secondary radiation from systems in resonance with the exciting light.[1-3] The problem seems to be particularly well defined for localized systems. In this case it is possible to define three types of secondary radiation; Raman scattering, resonance fluorescence, and hot luminescence. The distinction between Raman scattering and hot luminescence is made clear in Fig. 1. The spectra arising from these processes have similar properties. They both consist of a series of lines located at equal intervals from the exciting laser frequency.[4] However, for a localized electron-phonon system the two processes can be easily distinguished in the following ways. Hot luminescence involves a change in the quantum number of the localized mode associated with the excited electronic state, whereas Raman scattering involves the excitation of a ground-state phonon. Since the frequency of a localized mode is not, in general, the same in the ground and excited electronic states, the spacing between lines of a hot luminescence spectrum and of a Raman spectrum will not be the same. A more fundamental distinction is that the relative intensities of hot luminescence lines are determined by the anharmonic lifetime of the localized mode. For Raman scattering this lifetime plays no important role. In addition, the order dependence of the linewidths can also sometimes be used to distinguish these two processes.[5]

The distinction between resonant Raman scattering and resonant fluorescence is more subtle. If the energy of the exciting light is exactly that necessary to excite a vibrational level of the upper electronic state, emission of a photon takes place only after a measurable delay in time. For this case the scattering tensor is dominated by the contribution from an imaginary term. Such a process is called resonance fluorescence or sometimes even hot luminescence. In this paper, it will not be useful to distinguish between resonant Raman scattering and resonant fluorescence. However, a distinction will be made between resonant Raman scattering and hot luminescence as we have defined it.

These problems have been discussed in two previous papers[5,6] where multiple-order Raman scattering in additively colored CsI was reported. Although that system demonstrated up to 17-order scattering, it was not possible to measure a well-defined optical-absorption band. Much interesting work has been reported on resonant Raman scattering from F centers in alkali halides.[7-9] Although the F center has a well-defined optical-absorption band, the strong electron-phonon coupling washes out all vibronic structure. In order to observe the effects mentioned above it is necessary to work with a defect–host crystal system that has a well-defined vibronic absorption band in a frequency region accessible with dye lasers. Alkali halides doped with MnO_4^{2-} at substitutional sites satisfy this requirement.[10,11] Measurements of MnO_4^{2-} ions in aqueous solutions have already demonstrated that this ion has a large cross section for Raman scattering.[12] In this paper, we will report measurements of the optical and infrared absorption, Raman scattering, and resonant enhancement spectra of MnO_4^{2-} in CsI.

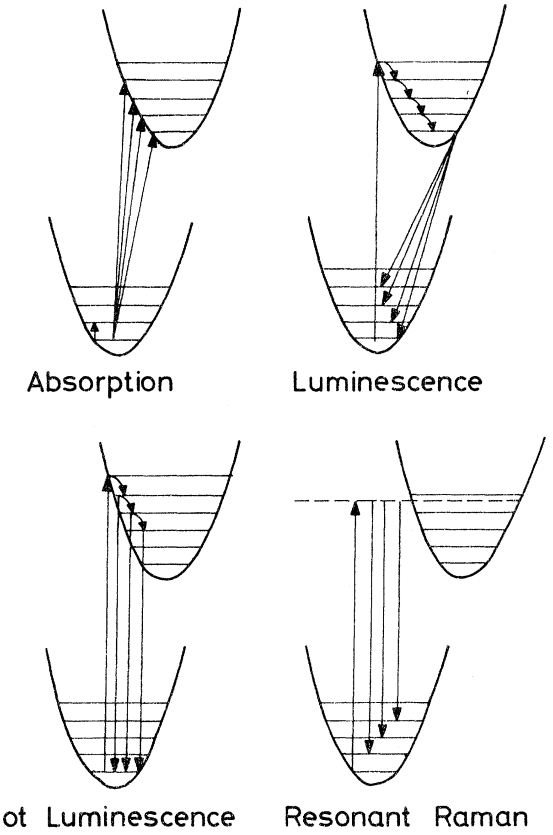

FIG. 1. Schematic representation of the energy levels and optical processes in a localized, coupled electron-phonon system. The lower parabola represents a ground electronic state with its vibrational sublevels; the upper parabola represents the excited electronic states. The straight arrows show absorption and emission of light, the curved arrows anharmonic decay of a localized mode into lattice phonons.

II. EXPERIMENT

The crystals were grown in air from a melt of CsI doped with 0.1-at.% MnI_2. Jain *et al.*[10] have established that KI crystals grown under these conditions contain MnO_4^{2-} ions at substitutional sites. From an atomic absorption analysis our crystals were found to contain 10–100-ppm manganese. Since no additional divalent positive impurity was added, charge compensation was probably achieved by the presence of negative-ion vacancies. CsI has a cubic lattice of the CsCl type. MnO_4^{2-} has a lower T_d symmetry. The symmetry of the defect system is lowered still more by the presence of the near-by charge compensating vacancy. Since CsI does not cleave well and since x-ray measurements on this material require very long exposure times, the crystals were oriented using stress-induced birefringence.[13]

The Raman measurements were made using a Jarrel-Ash double monochromator and photon counting detection. The light source was a Spectra-Physics dye laser pumped by a 4-W argon laser. Transmission measurements were made in the visible using a Cary 17 spectrometer and in the infrared using a Perkin Elmer 180 spectrometer.

III. RESULTS AND DISCUSSION

A. Optical absorption

The absorption coefficient of CsI:MnO_4^{2-} measured at 8 °K is shown in Fig. 2. Johnson[14] has performed a self-consistent-field scattered-wave calculation for the singly ionized form of this molecule and found that the lowest-energy dipole transition should be from a t_1 to an e orbital. The t_1 state is essentially a nonbonding oxygen $2p$ orbital. The e-level wave function is localized on the Mn atom and closely resembles a $3d$ state. In addition, Johnson has calculated the transition energy between these levels using occupation numbers halfway between the initial and final states in order to simulate relaxation effects. Since his calculated transition energy corresponds to 18 551 cm^{-1}; in reasonable agreement with our data, we feel it justified to assign the absorption to a t_1 to e transition.

The main absorption band contains substructure at equal intervals of 750 cm^{-1}. Each of these lines has a shoulder displaced by about 250 cm^{-1}. Such strong vibronic structure in optical spectra is almost always associated with a totally symmetric mode of vibration.[15,16] MnO_4^{2-} consists of a tetrahedron of oxygen surrounding a Mn atom in the center, i.e., it has T_d symmetry. The totally symme-

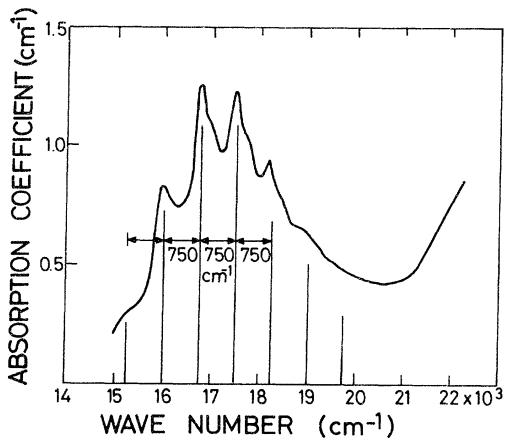

FIG. 2. Absorption coefficient of CsI:MnO_4^{2-} measured at 80 K. The main vibronic structure occurs at intervals of 750 cm^{-1}, The vertical bars represent the absorption coefficient calculated from Eq. (6) and (9) with $a = 3$. We have used a δ-function shape factor.

tric vibration involves the breathing motion of these oxygen atoms. In addition to this totally symmetric-A_1 mode, MnO_4^{2-} has two Raman-active E modes, three silent T_1 modes, and three triply degenerate T_2 modes which are both Raman and infrared active. This analysis includes translations and rotations of the ion in the crystal. This simple picture is complicated by the fact that the defect may have a neighboring vacancy which lowers the symmetry still further. However, the internal degrees of freedom are not expected to be greatly influenced by this perturbation on the environment.

From the optical-absorption curve we obtain two pieces of information which will be used later. First, the frequency of the A_1 mode of MnO_4^{2-} in the excited electronic states is 750 cm^{-1}. Second, we have established the position of vibronic structure. We might expect to see resonant enhancement of Raman scattering each time the incident photon energy coincides with the transition energy to one of the vibronic levels.

B. Raman spectra

The Raman spectrum CsI:MnO_4^{2-} is shown in Fig. 3. For this measurement the sample was cooled to 8 °K. The laser wavelength used, 5145 Å, is near but not at the center of the electronic absorption band. The spectrum is dominated by a series of sharp, almost equally spaced lines. Each sharp line can be seen to have a sideband containing considerable structure. The position, width, and integrated intensity of each of the sharp lines are listed in Table I. Notice that the frequency of the mode of vibration causing the series of sharp lines is about 800 cm^{-1}. The symmetry of this mode can be determined by observing the intensity of the line for various angles of polarization of the incident

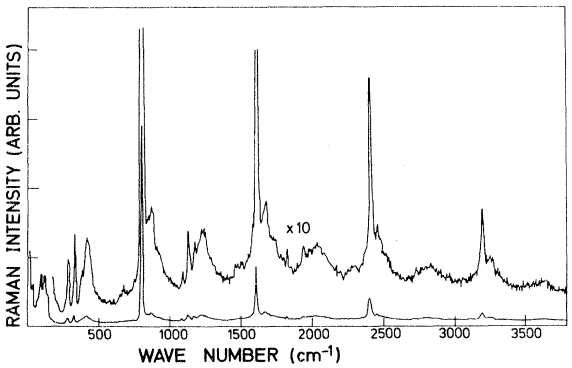

FIG. 3. Raman-scattering spectrum of CsI:MnO_4^{2-} measured at 80 K with 5145-Å Ar line. The four intense lines spaced at intervals of 800 cm^{-1} are multiple-order scattering from a localized mode. Each strong line exhibits a sideband.

TABLE I. Multiple-order Raman scattering in CsI:MnO_4^{2-}.

Order (n)	Position (ω_0) (cm^{-1})	ω_0/n (cm^{-1})	Width (cm^{-1})	Integrated intensity (arb. units)
1	803	803.0	7	1.00
2	1602.5	801.3	16	0.32
3	2400	800.0	30	0.16
4	3190	797.5	45	0.10
5	3980	796.0	105	0.09
6	4770	795.0	...	...

and scattered light. A scattering geometry was used with the incident light propagating along the [001] crystallographic axis z and the scattered light propagating in the [110] direction y. The symmetry of the phonons involved in the Raman process can be determined by measuring the $z(xx)y$, $z(xz)y$, and $z(yx)y$ spectra, where the symbols in parentheses refer to the polarization of the exciting and scattered light, respectively. The symmetry of the phonon causing the main series of lines proved to be A_1. The frequency of the A_1 mode observed in this Raman spectrum differs significantly from the frequency of the A_1 mode observed in the optical-absorption spectrum. That is, the frequencies of the ground-state and excited-state localized mode differ by 50 cm^{-1}. According to the definitions made in the introduction and depicted in Fig. 1, we can immediately conclude that the emitted light is resonant Raman scattering and not hot luminescence.

The frequencies of the first five intense Raman lines divided by the order are listed in column three of Table I. Clearly, the real part of the self-energy of the local mode increases with increasing excitation. If the widths of the Raman lines reflect the lifetimes of the vibronic states, i.e., if there is no inhomogeneous broadening, then the imaginary part of the self-energy can also be seen to increase with order. In a previous paper,[5] we have shown that for the case of additively colored CsI the principal anharmonic contribution to the linewidth comes from cubic anharmonicity, specifically, from the decay of the localized mode into two host-crystal phonons. However, for the manganate defect the maximum frequency of the host-crystal phonons, 90 cm^{-1}, is far below the localized mode frequency, 800 cm^{-1}. Energy can be conserved only if the local mode decays into ten or more host crystal phonons, a very improbable process. Therefore, the anharmonic processes must also involve lower-frequency internal vibrations of the MnO_4^{2-} molecule.

In addition to the series of equally spaced A_1

lines, the Raman spectrum in Fig. 3 contains several other features. The first 200 cm^{-1} of the spectrum is dominated by second-order Raman scattering from the host crystal CsI. This is followed by weak but sharp structure caused by Raman scattering from internal modes of vibration in the MnO_4^{2-}. This structure repeats itself in the form of sidebands of the intense A_1 lines. Although the intensity of the side bands decreases with order, the decrease is much less than that of the A_1 lines themselves. We have shown[5] that similar side bands in the Raman spectra of additively colored CsI are not anharmonic in origin but arise from a higher-order electron-phonon interaction. The higher order of the interaction can be used to explain the difference between the order dependence of the main line intensity and the sideband intensity. We assumed that the nth-order strong line can be described by a low-order electron-phonon interaction and $(n+2)$th- order perturbation theory, an assumption that is particularly good under resonant conditions. In order to describe the side band, an additional order of perturbation theory is needed, contributing not one but n distinct new scattering diagrams, i.e., the relative strength of the sideband is proportional to the order of the main line. The sideband of the first order A_1 line is shown more clearly in Fig. 4. Also indicated in this figure are the frequencies of weak lines seen in room-temperature infrared absorption measurements. Infrared measurements could not be made for frequencies below 250 cm^{-1} because of absorption by the host crystal. It can be seen that most of the modes seen in the Raman sideband are also infrared active. According to the symmetry analysis given at the beginning of this section only T_2 modes should be both infrared and Raman active. The results of polarized Raman measurements made on an oriented crystal also show that the indicated sideband lines have mainly T_2 symmetry. Host-crystal photons probably contribute to the sideband at frequencies below 90 cm^{-1}.

If the laser frequency coincides with a peak in the vibronic optical-absorption spectrum, we might expect an enhancement of the Raman scattering. In order to test this supposition the intensity of the first- and second-order Raman scattering was measured as a function of the frequency of the incident light from a tunable dye laser. The results of these measurements are shown by the circles in Fig. 5. In the frequency region accessible with the dye rhodamine 6G, two distinct peaks could be observed in the excitation of the first order Raman line. However, in the same frequency region three peaks could be seen in the optical absorption. One of the expected peaks in resonant enhancement is missing. In order to explain this result, we must now look at the problem in more detail. In Sec. III C the optical-absorption coefficient and Raman-scattering intensities of a localized system will be calculated using a configuration coordinate model.

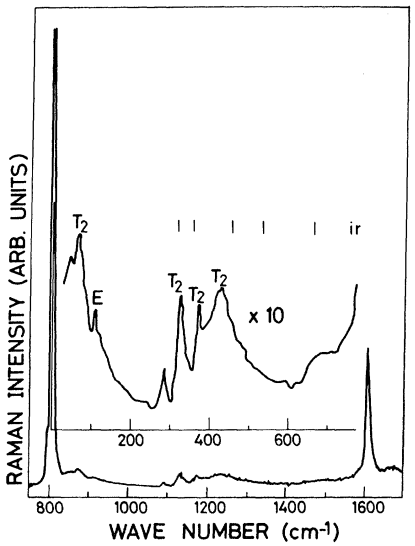

FIG. 4. Raman spectrum of $CsI:MnO_4^{2-}$ measured at 80 K showing the sideband of the first-order peak. The low-frequency structure is due to CsI phonons, the high-frequency structure to MnO_4^{2-} internal vibrations.

C. Calculation

The defect-induced absorption coefficient for a dipole transition from a ground state g to a final state f can be written[17]

$$\alpha(\omega) = (4\pi^2 q^2 N/3c)\,|\langle f|r|g\rangle|^2 \omega_{fg} S_{fg}(\omega), \qquad (1)$$

where N is the number of defects per unit volume,

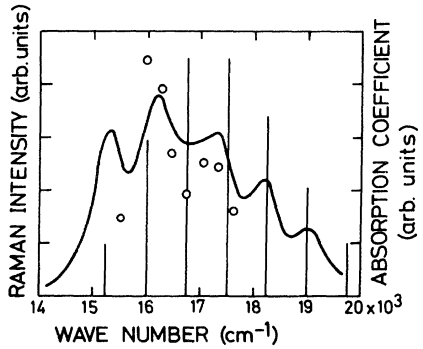

FIG. 5. Intensity of first-order Raman scattering of $CsI:MnO_4^{2-}$ as a function of laser frequency. The circles represent experimental points, the solid line a calculation. Notice that there is a minimum in the excitation spectrum at 16 750 cm^{-1} where there is a maximum in the absorption spectrum (vertical lines).

$\langle f|r|g\rangle$ is the dipole matrix element between the ground and excited states, and ω_{fg} and S_{fg} are the corresponding frequency and shape function. The effective charge is denoted by q. The Raman tensor can also be written in terms of dipole matrix elements[18]:

$$I_{jklm} = [n(\omega)+1]\langle g|P^*_{jk}|f\rangle\langle f|P_{lm}|g\rangle, \tag{2}$$

where j, k, l, and m are Cartesian coordinates, $n(\omega)$ is the thermal population number, and

$$\langle g|P_{jk}|f\rangle = \frac{q^2}{\hbar}\sum_e \frac{\langle g|r_j|e\rangle\langle e|r_k|f\rangle}{\omega_{ge}-\omega_l+i\Gamma} \tag{3}$$

plus an additional term which does not resonate. Here ω_l is the frequency of the incident light and Γ is determined by the lifetime of the states involved. We have summed over all intermediate excited states e. It can be seen that the determination of both the absorption coefficient and the intensity of Raman scattering reduces to the problem of evaluating dipole matrix elements. Several approximations must be made in evaluating this integral. The first is the Born-Oppenheimer approximation which assumes that the total wave function can be broken up into an electronic part depending parametrically on the phonon coordinates Q and a vibrational part dependent on the electronic quantum numbers but not explicitly on the electronic coordinates r. The matrix element can then be written

$$\langle g|r|e\rangle = \langle a\alpha|r|b\beta\rangle = \langle\alpha|\langle a|r|b\rangle|\beta\rangle, \tag{4}$$

where a represents the electronic quantum numbers of the ground state and α the vibrational quantum numbers of the ground state, while b and β are the corresponding quantum numbers of the intermediate state. The matrix element $\langle a|r|b\rangle$ can be expanded in phonon coordinates. Making the Condon approximation we assume that only the zero-order term is important. Then the dipole matrix element simplifies to

$$\langle a\alpha|r|b\beta\rangle = \langle a|r|b\rangle\langle\alpha|\beta\rangle. \tag{5}$$

Making these approximations in the expression for the absorption coefficient and for the Raman scattering we obtain

$$\alpha(\omega) = \sum_\beta \frac{4\pi^2 q^2 N}{3c}|\langle a|r|b\rangle|^2\,|\langle\alpha|\beta\rangle|^2\omega_{a\alpha,b\beta}S_{a\alpha,b,\beta}(\omega) \tag{6}$$

and

$$\langle a\alpha|P_{jk}|a\alpha'\rangle = q^2\langle a|r_j|b\rangle\langle b|r_k|a\rangle \times\sum_\beta \frac{\langle\alpha|\beta\rangle\langle\beta|\alpha'\rangle}{E^0+\beta\hbar\omega_b-\hbar\omega_l+i\Gamma}, \tag{7}$$

where ω_b and ω_l are the excited-state vibrational frequency and the laser frequency, respectively. The zero-phonon energy has been written E_0. In writing down these expressions several additional approximations have been made. At low temperature only one state, $a\alpha$, is populated. There exists only one excited electronic state b. However, this state has several vibrational sublevels β.

We see that the frequency dependence of the absorption, Raman, and excitation spectra is not influenced by the electronic dipole matrix element but is determined by vibrational overlap integrals. A calculation of the complete set of vibrational wave functions for both the ground and excited state is a difficult problem. However, the task is somewhat simplified for a localized defect where the number of degrees of freedom is limited. The total electronic energy can be expanded in powers of one vibrational mode coordinate Q. If Q is defined to be zero at the equilibrium position of the ground state, then

$$E_a = E_a^0 + \tfrac{1}{2}m\omega_a^2Q^2 + \cdots. \tag{8}$$

However, the excited state does not necessarily have the same equilibrium position, so

$$E_b = E_b^0 - a\hbar\omega_b(m\omega_b/\hbar)^{1/2}Q + \tfrac{1}{2}m\omega_b^2Q^2, \tag{9}$$

that is, the vibrational part of the ground and excited states can be represented by harmonic oscillators with different frequency and different equilibrium positions. We will make the further assumptions that the eigenfrequencies are the same. The overlap integral between the vibrational wave functions in the ground and excited state can then be written[19]

$$\langle\alpha|\beta\rangle = e^{-a^2/4}(\alpha!/\beta!)^{1/2}(a/\sqrt{2})^{\beta-\alpha}L_\alpha^{\beta-\alpha}(\tfrac{1}{2}a^2), \tag{10}$$

where L is a Laquerre polynomial. Now we are in a position to calculate the optical-absorption coefficient and the Raman tensor. First consider the absorption coefficient. At sufficiently low temperature only the lowest vibrational level will be populated in the initial state, that is, α is equal to zero. In this case Eq. (10) simplifies to

$$|\langle 0|\beta\rangle|^2 = e^{-a^2/2}(\tfrac{1}{2}a^2)^\beta/\beta! \tag{11}$$

We have one parameter a to fit the relative absorption due to the various vibrational levels β. Using the value $a=3.0$, reasonably good agreement with experiment can be obtained as seen in Fig. 2. For clarity in this figure, the shape function, $S(\omega)$ in Eq. (1), has been assumed to be a δ function. The use of a Lorentzian shape function with a width Γ equal to 400 cm^{-1} results in a good fit to the shape of the experimental absorption spectrum.

There is an apparent inconsistency in our model for the electron-phonon interaction. Experimentally, we have shown there exists a clear difference

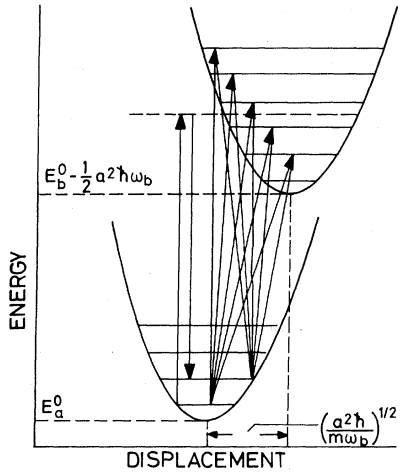

FIG. 6. Schematic representation of first-order Raman scattering from a localized defect. Several of the virtual absorption-emission processes contributing to the first-order scattering are shown on the right-hand side.

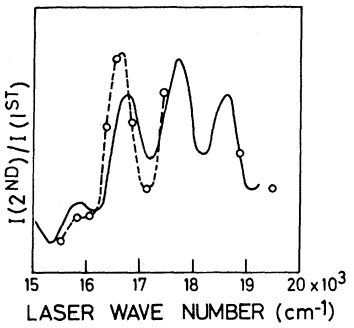

FIG. 7. Ratio of the intensity of second-order Raman scattering to the intensity of first order for CsI:MnO_4^{2-} as a function of laser frequency. The circles and dotted line indicate measured values, the solid line calculated values.

in the localized mode frequency for the ground and for the excited electronic state. However, in Eq. (10), the expression for the overlap integrals, we have assumed that these frequencies ω_a and ω_b are equal. Keil[20] has made explicit calculations for the contribution to the overlap integrals for the case ω_a unequal to ω_b in terms of a parameter $x = (\omega_b - \omega_a)^2/(\omega_b + \omega_a)^2$. His calculations show that this quadratic electron-phonon interaction contributes to the absorption only if $\beta - \alpha$ is an even integer and that this contribution decreases monotonically with increasing $\beta - \alpha$. Such a contribution to the absorption is not compatible with the experimental result. For the relatively small value of x appropriate for our system, the contribution can, in fact, be shown to be negligibly small.

Now it is possible to calculate the dependence of the intensity of Raman scattering on laser frequency without introducing any additional parameters. We have evaluated the matrix element defined by Eq. (7). The necessary overlap integrals were determined numerically using Eq. (10). The summation was made over the first seven intermediate states β. The virtual absorption and reemission processes appropriate for first-order Raman scattering are shown in Fig. 6. Since the signs of the overlap integrals depend on the states involved, contributions from the various virtual processes can interfere either constructively or destructively. In fact, it is just such an interference effect that explains why the absorption peak at 16 750 cm^{-1} was not reproduced in the experimental excitation spectrum. Interference effects were included in the calculated intensity for first-order Raman scattering shown by the solid curve in Fig. 5. We see that the calculated intensity is not a maximum at 16 750 cm^{-1} but a minimum in agreement with the experimental result.

When measuring the excitation spectrum for Raman scattering it is always a problem to make accurate corrections for absorption of the incident light. A particularly simple solution to this problem can be found when measuring multiple-order Raman scattering. By measuring the ratio of the intensity of the second-order to first-order scattering, corrections for absorption and laser power are not needed. Such measurements for CsI:MnO_4^{2-} are shown in Fig. 7 and compared with a calculation based on Eqs. (2), (7), and (10). Considering that this calculation has no free parameters the agreement with experiment is quite good. In summary, we have observed Raman scattering in resonance with vibrational sublevels of the excited electronic state of an impurity. The excitation spectrum showed interference among the individual contributions from these sublevels. These results could be explained quantitatively using a configuration coordinate model to describe the electron-phonon interaction.

---

*On leave from the Institute for Optical Research, Kyoiku University, Sinzyuku-ku, Tokyo, Japan.

[1]K. Rebane and P. Saari, J. Lumin. 12/13, 23 (1976).
[2]Y. R. Shen, Phys. Rev. B 9, 622 (1974).
[3]R. M. Martin and L. M. Falicov, in *Light Scattering in Solids*, edited by M. Cardona (Springer, Berlin, 1975).
[4]For the case of hot luminescence, this behavior requires a small but ever present amount of inhomogeneous broadening.
[5]T. P. Martin, Phys. Rev. B 13, 3617 (1976).

[6]T. P. Martin, Phys. Rev. B 11, 875 (1975).
[7]J. M. Worlock and S. P. S. Porto, Phys. Rev. Lett. 15, 697 (1965).
[8]C. J. Buchanauer, D. B. Fitchen, and J. B. Page, in *Light Scattering Spectra of Solids*, edited by G. B. Wright (Springer, New York, 1969).
[9]D. S. Pan and F. Lüty, in *Light Scattering in Solids*, edited by M. Balkanski, R. C. C. Leite, and S. P. S. Porto (Flammarion, Paris, 1976).
[10]S. C. Jain, S. K. Agarwal, and G. D. Sootha, J. Phys. Chem. Solids 32, 897 (1971).
[11]R. Singh and S. K. Agarwal, J. Phys. Chem. Solids 36, 1073 (1975).
[12]W. Kiefer and H. J. Bernstein, Mol. Phys. 23, 835 (1972).
[13]K. Maier, J. Cryst. Growth 6, 111 (1969).
[14]K. H. Johnson, Adv. Quantum Chem. 7, 143 (1973).
[15]E. V. Doktorov, I. A. Malkin, and V. I. Man'ko, J. Phys. B 9, 507 (1976).
[16]M. D. Frank-Kamenstskii and A. V. Lukashin, Usp. Fiz. Nauk 116, 193 (1975) [Sov. Phys.-Usp. 18, 391 (1976)].
[17]D. L. Dexter, in *Solid State Physics*, edited by F. Seitz and D. Turnbull (Academic, New York, 1966), Vol. 6.
[18]A. D. Albrecht, J. Chem. Phys. 34, 1476 (1961).
[19]P. P. Shorygin, Usp. Fiz. Nauk. 109, 293 (1973) [Sov. Phys.-Usp. 16, 99 (1973)].
[20]T. H. Keil, Phys. Rev. 140, A601 (1965).